

## Seismic velocity structure beneath southern Hokkaido and its relation to crustal deep low-frequency earthquakes

\*Takahiro Shiina<sup>1</sup>, Hiroaki Takahashi<sup>1</sup>, Tomomi Okada<sup>2</sup>, Toru Matsuzawa<sup>2</sup>

1. Institute of Seismology and Volcanology, Graduate School of Science, Hokkaido University, 2. Research Center for Prediction of Earthquakes and Volcanic Eruptions, Graduate School of Science, Tohoku University

The crustal deep low-frequency earthquakes (CDLFE) are often occurred beneath active volcanoes in Japan (e.g., Takahashi and Miyamura, 2008). Additionally, some CDLFEs showing the similar characteristics for those observed beneath volcanoes are also detected in non-active volcanic areas, such as a fault zone (e.g., Ohmi and Obara, 2002). However, relations between the CDLFEs and volcanoes and regular earthquakes occurred in the arc crust have not been revealed in clearly.

In southern Hokkaido, the CDLFEs are observed beneath both of active volcanoes and non-active volcanic areas, which corresponds to shallow swarm-like activity of the regular crustal earthquakes. This indicates southern Hokkaido is an interesting region for understanding the relations between the CDLFE and near surface phenomena, including volcanoes and crustal earthquakes. In this study, therefore, we investigate seismic velocity structure beneath southern Hokkaido in detailed and then discuss the relations of them based on the obtained heterogeneous structure.

In order to estimate the seismic velocity, we applied the double-difference tomography technique (Zhang and Thurber, 2003; 2006). From the earthquake catalogue by Japan Meteorological Agency, we collected 15,645 earthquakes which occurred in the period from March 1st, 2003 to June 15th, 2016. A magnitude range of the earthquakes was 1.5-6.5. The number of travel time data is 306,335 for P wave and 242,093 for S wave.

In addition to characteristic structures as imaged in previous studies (e.g., Kita et al., 2010; Niu et al., 2016), the obtained results clearly show the low-velocity zones are distributed at depths of about 20-40 km beneath around the active volcanoes and generating regions of the CDLFEs. Correspondingly, high- $V_p/V_s$  ratio is calculated at the depths. In contrast, high-velocity zones are widely determined at a depth of 10 km, while reductions of seismic velocity from surroundings are obtained near the active volcanoes. The crustal earthquakes which involves shallow seismic swarms occurred above the DLFES seems to be located within the high-velocity zones. The obtained spatial variations of the seismic velocity demonstrate that the CDLFEs are posited at transition zones of velocity and  $V_p/V_s$  ratio, proposing that presence and migration of fluids or melts would attribute for their triggering (e.g., Ukawa and Ohtake, 1987). Additionally, heterogeneity that associate with the upper crust and correspond to the CDLFEs seem to closely link to the subsurface phenomena at above the CDLFEs: crustal earthquakes occurred in the upper crust are facilitated in the high-velocity zones and active volcanoes are located within the low-velocity area those compared from surroundings.

Keywords: seismic velocity, deep low-frequency earthquakes, seismic swarm, Hokkaido

# The 2016 Northern Ibaraki Prefecture Earthquake ( $M_j$ 6.3) Rupturing the Fault of the Large Earthquakes in 2011 Again

\*Takahiko Uchide<sup>1</sup>, Makiko Ohtani<sup>1</sup>, Miki Takahashi<sup>1</sup>, Kazutoshi Imanishi<sup>1</sup>

1. Geological Survey of Japan, National Institute of Advanced Industrial Science and Technology (AIST)

The 2011 Tohoku-oki earthquake ( $M_w$  9.0; hereafter referred to as "mainshock") activated the seismicity in many areas not only in Japan but also all over the world. In particular, in the Fukushima Hamadori and the northern Ibaraki prefecture (hereafter, "N. Ibaraki") areas, northeast Japan, the rate of the seismicity with normal faulting mechanisms jumped to high, although the seismicity had been inactive before the mainshock. This is because the preexisting east-west extensional stress regime was significantly strengthened by the mainshock [Imanishi *et al.*, 2012]. In the N. Ibaraki area, a large earthquake with Japan Meteorological Agency magnitude ( $M_j$ ) of 5.7 ("Event 2011a") occurred just 8 minutes after the onset of the mainshock. Another large earthquake ( $M_j$  6.1; "Event 2011b") struck on March 19, 2011, 8 days after the mainshock. On April 11, 2011, an  $M_j$  7.0 earthquake struck the Fukushima Hamadori area, on the north of the N. Ibaraki area. Afterward the seismicity has been attenuating with time.

On December 28, 2016, a large earthquake ( $M_j$  6.3, "Event 2016") occurred in the N. Ibaraki area. The interferograms of the SAR data for Events 2011a and 2011b [Kobayashi *et al.*, 2011] and Event 2016 [Geospatial Information Authority of Japan (GSI), 2017] are very similar to each other, implying the similarity in earthquake rupture processes.

We analyzed rupture processes of the Events 2011a, 2011b, and 2016 by finite-fault slip inversion analyses using strong-motion data from KiK-net, K-NET, and F-net. Our fault models indicate that the Events 2011a and 2016 ruptured the ground surface as reported by field observations [Aoyagi *et al.*, 2015; Geological Survey of Japan, 2017], whereas Event 2011b did not. Note that this does not contradict the SAR analysis [Kobayashi *et al.*, 2011] and the field observation [Aoyagi *et al.*, 2015], because they have no temporal resolution to distinguish the deformation occurred on March 11 (Event 2011a) and 19 (Event 2011b). Overall the rupture areas of two events in 2011 and the Event 2016 are overlapping and similar to each other.

Why could the large earthquakes occur on the same fault twice in such a short time, almost 6 years? Since the fault strength recovers quickly [e.g., Dieterich, 1972], a stress loading and/or a fault weakening are required. According to the strain change inferred from the GNSS data by GEONET of GSI, the east-west extensional plain strain on the ground surface was rapidly increased after the mainshock, however afterward the east-west compressional strain rate has been observed, which seems to contradict the occurrence of the normal faulting large earthquake. Detail will be studied by a seismicity analysis based on the ETAS model [Uchide, this meeting].

It is probable that the large earthquakes in the N. Ibaraki area occurred due to the coseismic and postseismic deformation of the Tohoku-oki mainshock. Since the postseismic deformation generally attenuate with time, the seismic activity will also be decay. A quantitative assessment will require numerical simulations with a precise rheology model as well as seismic and geodetic observation to monitor the seismicity and crustal deformation.

Keywords: Northern Ibaraki Prefecture Area, Inland Earthquake

## Very short recurrence interval of M $\sim$ 6 earthquakes within the common fault zone

\*Aitaro Kato<sup>1</sup>, Shin'ichi Sakai<sup>1</sup>, Takashi Iidaka<sup>1</sup>, Kazushige Obara<sup>1</sup>

1. Earthquake Research Institute, the University of Tokyo

Immediately after the 2011 M9.0 Tohoku-Oki, an intensive seismicity characterized as normal faulting was induced near the Pacific coast in the southern part of Tohoku region [Kato et al., 2011, 2013]. From the end of March in 2011 to the present, we have continued to precisely monitor the seismicity deploying a dense seismic network consisting of around 60 portable stations equipped with short-period sensors (the station interval is around 4 km). The seismicity has continued after the Tohoku-Oki earthquake, while the seismicity rate has gradually decreased. On 28 December, 2016, a magnitude of 6.3 earthquake took place in this region, and boosted up an intensive seismicity. We relocated aftershocks following this event, using seismic waveforms retrieved from the dense seismic network. The relocated earthquakes almost overlapped with those triggered after M6.1 earthquake on 19 March, 2011. A sharp alignments of earthquakes dipping toward SW was clearly imaged. This indicates that two magnitude 6 earthquakes occurred on the common fault zone. This idea is supported by spatial pattern of surface displacements revealed by InSAR technique (GSI, 2017). It is very surprising that M6 earthquakes took place with very short recurrence interval along the common fault zone.

# Estimation of spatiotemporal distribution of interplate slip after the 2003 Tokachi-oki earthquake incorporating viscoelastic relaxation

\*Yuji ITOH<sup>1</sup>, Takuya NISHIMURA<sup>2</sup>

1. Graduate School of Science, Kyoto University, 2. Disaster Prevention Research Institute, Kyoto University

The 2003  $M_w$  8.0 Tokachi-oki earthquake is an interplate earthquake along the Kurile trench. Its postseismic deformation has been observed by GNSS [e.g., Miyazaki et al. 2004]. Estimation of spatiotemporal afterslip is a key to clarify the healing process after large earthquake. Because the postseismic deformation should be caused by both viscoelastic relaxation and afterslip, it is important to incorporate both effects for the modeling. In this study, we estimated a spatiotemporal interplate slip for about 7.5 years following the 2003 event as well as the coseismic slip of the 2003 and M 6-7 class earthquakes simultaneously. We included a viscoelastic response of interplate slip in the estimation of the slip.

For the data analysis, we corrected the effect of the 1993 Hokkaido-Nansei-oki earthquake for the observed GNSS data in Hokkaido by using the model of Ueda et al. [2003]. The secular velocity before the 2003 event was estimated from the corrected data and removed from the postseismic data. And then, we removed a seasonal variation and displacements of the M6-7 events in the postseismic period. Finally, we down-sampled the residual time series with an interval of 1-6 months. We used about 7.5 years long GNSS data until the 2011 Tohoku-oki earthquake.

For the modeling of postseismic deformation, we constructed a model consisting of the coseismic slip of the 2003 and the following M6-7 class events, interplate slip including afterslip following these events and viscoelastic relaxation. We assumed the two-layers viscoelastic structure estimated by Itoh and Nishimura [2016] to estimate interplate slip distribution.

A preliminary result shows large postseismic slip occurred in the up-dip and down-dip extensions of the coseismic slip region and implies an interplate coupling had not been recovered to that before the 2003 event at the time of the 2011 event.

Keywords: The 2003 Tokachi-oki earthquake, GNSS, Postseismic deformation, Afterslip, Viscoelastic relaxation

# Toyama Trough Shear Zone of Japan Sea and active tectonics along Japan margin of Amur Plate

\*Akira Takeuchi<sup>1</sup>

1. Faculty of Science, University of Toyama

In Japan, crustal earthquakes continue to occur along strain-concentrating zones on the Japan Sea side and inland Honshu since the 1995 Hyogo-ken-Nanbu earthquake. In addition, following the occurrence of the 2011 off the Pacific coast of Tohoku Earthquake, trench-type interplate earthquakes and intraplate crustal earthquakes in the inner belt of the island arc have been discussed widely. Moreover, marine resource development based on the national Basic Plan on Ocean Policy, crustal structure survey integrating land and sea areas, earthquake / geodetic observation, etc. were carried out densely and data accumulated.

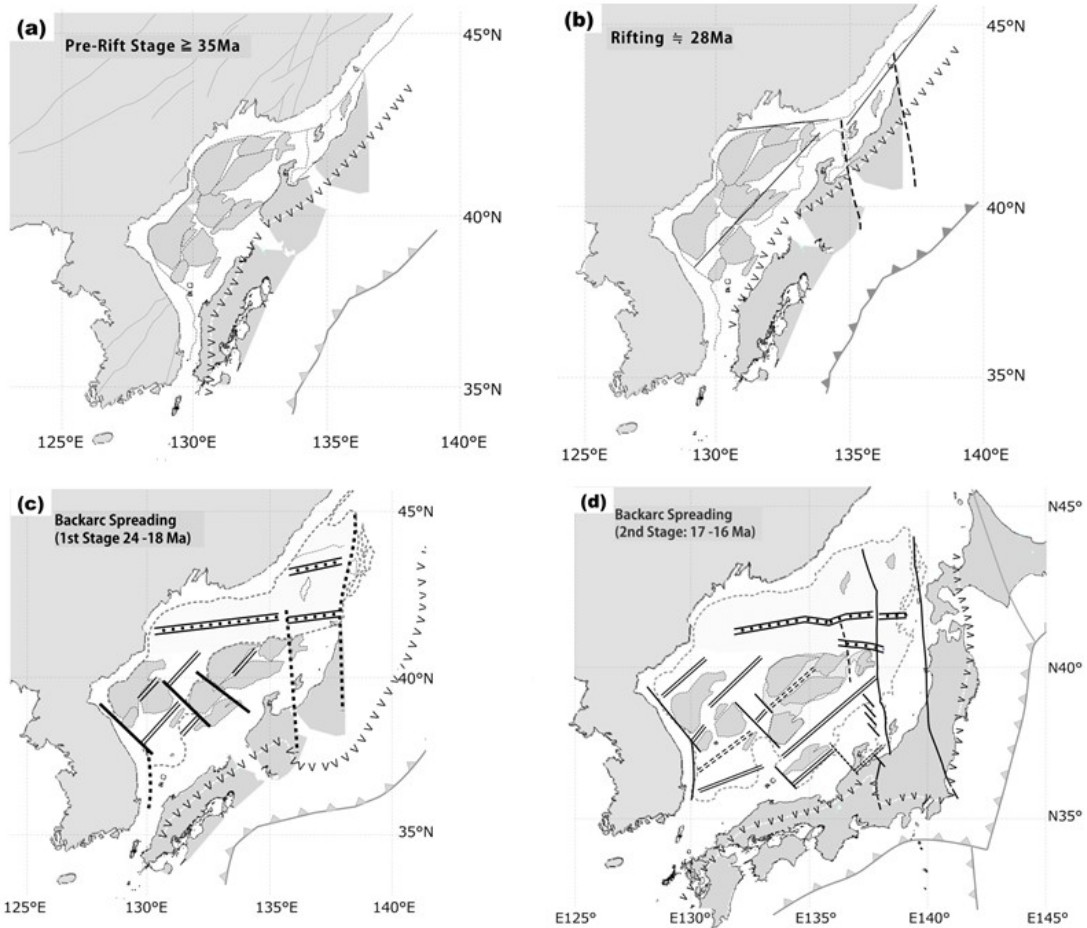
This paper re-analyzed and elucidated the geologic structure and its development along the eastern margin of Japan Sea, including the southeastern Japan Basin, the eastern Yamato Basin and Toyama Trough, based mainly on the recent data sets of seismic investigations for resource-exploring and earthquake disaster prevention. The obtained results corroborate a two-stage model of the back-arc spreading with large shear zone in a north-south trend along the eastern border of Japan Basin and Yamato Basin.

The new findings were as follows:

- 1) Regional geologic structure, including not only the present-day active faults but also the suspended Miocene faults, in the reactivated Honshu arc and its back-arc basin became clear.
- 2) The N-S striking system, one of three fault systems observed in the present Toyama Trough, was traced not only southerly along the Itoigawa-Shizuoka tectonic line, but also northerly up to the eastern termination of Yamato Basin.
- 3) During the time of a clockwise rotation at around 17 Ma in southwestern Japan, the 2nd stage of back-arc spreading occurred in and around Yamato Basin. The Toyama Trough shear zone was widespread with being accompanied by NW-SE trending left-lateral strike-slip faulting.
- 4) A shift to a convergent mode was revolutionary as neotectonics in Central Japan from a divergent mode in the Japan Sea. Such a conversion was different in style and occurring time: E-W trending folds occurred in the Late Miocene at Noto Peninsula on the Southwest Japan arc side, probably under the effect of subduction of Philippine Sea Plate. The NE-SW trending fault/fold structure characterizing the southern Toyama Trough and the Shin-Etsu sedimentary basin on the Northeast Japan arc side is further delayed to become conspicuous after 4Ma, probably due to commencement of eastward motion of Amur Plate.
- 5) Based on the aspect of relative movement along the plate boundary between Amur and Okhotsk, the diversity of fault distribution of the target area is regarded as a combination of the "colliding side" and the "passive side" among the domain of island arc-arc collision along the Toyama Trough shear zone. On the collided side, "Normal inversion" excels dominantly throughout the inner zone of Northeast Japan arc including the eastern margin of the Japan Sea Basin. While on the colliding side, "conversion-in-sense-of-faulting" occurs in the inland of the Southwest Japan arc associated with the reactivated late-Cretaceous faults, and "anti-inversion" is seen in the back-arc basin. In the Yamato Trough, re-activity of the Miocene normal faults involved in the sea floor spreading is not recognized.
- 6) The Present strain concentration belt in Honshu, the Niigata-Kobe tectonic zone, is observed extended over along the Japan Sea side on the Northeast Japan arc through an inland area of the Southwest Japan

arc, intersecting with the Itoigawa-Shizuoka tectonic line. Its manifestation in the late Quaternary time could be called as "revival Honshu arc" as a behavior of collision and coalesce of the two island arcs, Northeast and Southwest Japan arcs, concerning the interaction of the subducting Pacific Plate with the hanging two plates.

Keywords: Japan Sea, neotectonics, Toyama Trough, tectonic inversion, Amur Plate



A tectonic scenario explaining a progressive opening of Japan Sea and rotation of Southwest Japan

# Deformation of the Philippine Sea Slab and its Implication for the Tectonics of Central and Western Japan

\*Yukitoshi Fukahata<sup>1</sup>

1. Disaster Prevention Research Institute, Kyoto University

In this study, I estimate the contraction rate in central and western Japan from deformation of the Philippine Sea slab. Usually a slab subducts with little deformation as indicated by the slab contour lines that are nearly parallel to the trench in most subduction zones. Little deformation of slabs is reasonable from the view point of elastic energy.

However, the Philippine Sea slab is an exception; large deformation of it beneath central Japan has been estimated from hypocenter distributions, receiver function analyses, and seismic waveform tomography. It is considered that such large deformation is caused by east-west contraction, which prevails in the most area of Japanese islands.

Observed characteristics of the deformation of the Philippine Sea slab are as follows: (1) little deformation in the west of the Kii strait; in the east of the Kii strait, (2) little deformation in the region between the Nankai trough and the coast line, (3) progressively accumulated deformation to the north of the coast line. Little deformation in the west of the Kii strait is consistent with less number of active faults and their commonly slow displacement rates.

The deformation rate of the Philippine Sea slab related to the characteristic (3) is estimated to be about 5 - 10 km/Ma. This estimate would give the minimum contraction rate in the crust of the Chubu and Kinki district, Japan.

Keywords: Philippine Sea slab, crustal deformation, central Japan



# The characteristics of the brittle deformation structure causing “Crustal strain-rate paradox” in the Niigata-Kobe Tectonic Zone

\*Tomonori Tamura<sup>1</sup>, Kiyokazu Oohashi<sup>1</sup>

1. Yamaguchi University Graduate School of Sciences and Technology for Innovation

## Introduction

NKTZ has been known as the high strain rate zone causing right lateral movement and the slip rate of the zone is estimated to 12mm/y by GNSS observation (Ohzono et al., 2011). On the other hand, the total slip rate based on geological survey of the active faults in the NKTZ (the Atostugawa fault, Ushikubi fault and Takayama-Oppara fault) is only 6mm/y. This result is not equal to the result of the GNSS observation. This is called “Crustal strain-rate paradox”. However, the rate of the Kokufu fault zone which is distributed in the southward area of the Atostugawa fault system is not considered when discussing this paradox. The Kokufu fault zone has not yet been investigated by the topographic or geological survey in detail and clarified the brittle deformation structure. The aim of this study is to clarify the brittle deformation structure in and around the Kokufu fault zone by using topographic and geological approaches and discuss what causes the paradox in the NKTZ.

## Topographic and Geological Overview

In the study area, active faults such as Unehata fault and Toichigawa fault which is belonging to the Kokufu fault zone are distributed. There are also fault taraces indicating active faults in the Inagoe area. The Hida metamorphic rocks, Tedori formation, Nohi rhyolite, Funatsu granite are distributed in the study area. According to geological map (Geological Survey in Japan, 1975) in the study area, there are many geological faults or geological boundary faults.

## Results

In the Miborotani outcrop (Loc.1), the fault is composed of 10 cm yellow-orange fault gouge and fault breccia. Strike and dip of the fault gouge is N65E85S and the plunge of the slickline on the fault surface plunges 10 to the south. This fault outcrop is composed of Unehata fault.

In the Kurigatani outcrop (Loc.2), the fault is composed of 20 cm blue gray fault gouge and fault breccia. Strike and dip of the fault gouge is N25E60S and of the slickline on the fault surface plunges 18 to the south. This fault outcrop is in the area located about 200 meters far away from the active faults.

In the Soutsuitani outcrop (Loc.3), the fault is composed of the fracture zone including fault gouge and fault breccia. Strike and dip of the fracture zone is N89W75N.

## Discussion

By the topographic and geological surveys, we found many faults in the off-fault area which is the area far away from the active faults. These faults cause the “Crustal strain-rate paradox”. Therefore, it is important for considering “Crustal strain-rate paradox” to clarify the brittle deformation structure around the Kozkufu fault zone.

Keywords: Niigata-Kobe Tectonic Zone, brittle deformation structure

## Temporal variation in Coda Q in the northeastern part of Niigata-Kobe Tectonic Zone in 2009-2014

\*Masanobu Dojo<sup>1</sup>, Yoshihiro Hiramatsu<sup>2</sup>

1. Graduate school of Natural Science and Technology, Kanazawa University, 2. Faculty of Natural System, Institute of Science and Engineering, Kanazawa University

Large earthquakes modulate the stress state in the crust, resulting a temporal change in seismicity and/or heterogeneity of the crust. Hiramatsu et al. (2000) and Sugaya et al. (2009) reported a temporal change in coda Q in Tamba region associated with the 1995 Hyogoken-Nanbu earthquake. Padhy et al. (2013) also reported a temporal change in coda Q along the Pacific coast of Tohoku caused by the 2011 Tohoku earthquake. However, Tsuji et al. (2014) reported no statistically significant temporal change in coda Q around the Nobi fault zone, the central part of the NKTZ due to the 2011 Tohoku earthquake. We investigate here details of the temporal variation of coda Q in the northeastern part of the NKTZ during January 2009 to February 2011 (period I) and January 2012 to October 2014 (period II).

We have analyzed 646 events in the period I and 2194 events in the period II in the northeastern part of the NKTZ. Those magnitudes are greater than 1.8 and the depths shallower than 30 km. For each station, we select events of which epicentral distance are within 30 km for the analysis of coda Q. We applied the single back-scattering model (Aki and Chouet 1975) for the estimation of coda Q.

We compare the obtained coda Q between the periods I and II. The change in  $\log(\text{coda } Q^{-1})$  is smaller than 13% between the periods I and II. We investigate the spatial variation of the change between the periods I and II. Spatial distributions of increase  $\log(\text{coda } Q^{-1})$  variation at 1-2 and 2-4 Hz frequency bands is volcanic area and it is difficult to find a distinct pattern of the spatial distribution of  $\log(\text{coda } Q^{-1})$  variation at 4-8, 8-16, and 16-32 Hz frequency bands that is related closely to the fault zones, volcanic area, or the high strain rate zone. We apply t tests to analyze the significance of these temporal variations and find that little variations are statistically significant. These facts imply that the temporal variation in coda Q caused by the 2011 Tohoku earthquake is not significant in this study area.

Keywords: the 2011 Tohoku earthquake, high strain rate zone

# Tectonic Loading of the Atera Fault inferred from Dense GNSS Observation

\*Koki Kumagai<sup>1</sup>, Takeshi Sagiya<sup>2</sup>, Nobuhisa Matsuta<sup>3</sup>

1. Earthquake and Volcano Research Center Graduate School of Environmental Studies, Nagoya University, 2. Disaster Mitigation Research Center, Nagoya University, 3. Okayama University Graduate School of Education

The Atera Fault is in the east of Gifu Prefecture is a major active fault in Japan. The fault is left-lateral strike slip in the NW-SE direction, consistent with E-W trending P-axes of earthquakes. The geological slip rate is 2~4mm/year and the seismic recurrence interval is estimated to be about 1700 years. However, a hydraulic fracturing experiment and the GEONET F3 solution suggested the Atera Fault undergoes right-lateral displacement (Yamashita et al. 2010), which is not consistent with the long-term activity of the fault. In this study, We study crustal deformation and stress field of the Atera Fault by GNSS observation and numerical modeling. For this purpose, we install using dense GNSS network near the fault trace with an average interval of several kilometers in order to reveal detailed crustal deformation pattern. Based on GNSS daily coordinate from is January 2014 to October 2016, we calculate average horizontal velocity at each GNSS site. The velocity pattern is dominated by the postseismic deformation of the 2011 Tohoku-oki earthquake and interplate coupling at the Nankai Trough. Therefore we correct overall deformation pattern in order to extract displacements related the fault activity. After the correction, a left-lateral displacement pattern is identified. Then I conclude the Atera Fault is dislocating left-lateral. Comparison with the elastic dislocation model showed that our observation is consistent with geological estimated fault slip rate (2~4mm/year) and the seismologic layer thickness (~15km) in central Japan. We also evaluate the topographic perturbation on the crustal stress field under a lithostatic equilibrium. The calculation suggests that the topographic effect is significant at shallow depth (~5km) and greatly affects the crustal stress pattern. The calculated maximum compressional axis at the hydraulic fracturing site depth of 350m is directed to the north-south with a differential stress of about 1.70~3.86MPa, consistent with the observation. The results demonstrate that the motion of the Atera Fault is left-lateral, consistent with the regional stress field. It is also suggested that tectonic loading of a crustal fault does not change even under elastic perturbation due to postseismic deformation and interplate coupling. It is essential to estimate stress field at the seismogenic depth in order to discuss fault activity.

Keywords: Atera Fault, GNSS, Tectonic Loading, stress, Boussinesq

## Strain concentration zone in the San-in area analyzed by GNSS data

\*Tsukasa MITOGAWA<sup>1</sup>, Tetsuya KOGURE<sup>1</sup>

1. Interdisciplinary Faculty of Science and Engineering, Shimane University

Micro-earthquakes are distributed along the coast of the Japan Sea in the San-in area located in the north of the Japan Median Tectonic Line. Large earthquakes such as the 2000 Tottori Western Earthquake (M7.3) and the 2016 Middle Tottori Earthquake (M6.6) occurred in this area. Both earthquakes occurred along unidentified faults. This suggests that the information about the distribution of active faults is not enough to predict the occurrence place of earthquakes.

GNSS Earth Observation Network System (GEONET) was launched by the Geospatial Information Authority of Japan (GSI) in 1994. GEONET revealed the pattern of the surface crustal movement. Sagiya et al. (2000) used the technique and found Niigata-Kobe Tectonic Zone (NKTZ) where strain rate was large. Actually, many earthquakes occur along this zone. Therefore, strain rate in San-in area is also expected to be large. The purpose of this study is to find strain concentration zones in the San-in area considering the distribution of strain rate in high resolution calculated from GNSS data.

We used the GNSS daily coordinates (so-called the GEONET F3 solution) provided by GSI (Nakagawa et al., 2009). We calculated only the trend component of displacement rate although GNSS data itself includes the effects of some parameters such as annual and semi-annual trend of deformation or step deformation due to earthquakes. The displacement rate at each observation point was aligned to lattice point with interval of 0.1 degree obtained by Nearest Neighbor method in Generic Mapping Tools (GMT). The maximum rate of shear strain was calculated by differentiating displacement rate with respect to the distance among each lattice point. Results show that the distribution pattern of the strain rate changes with time and observation period. The largest strain rate of about 200 nanostrain/yr is found in Middle Tottori and around Mt. Sambe, which is an active volcano in Middle Shimane.

Keywords: Strain rate, GNSS, San-in area

## Fault distribution in the southern part of the small earthquake swarm zone along the Sanbe to Miyoshi, central Chugoku region, Japan

Takeshi Nagira, Hideto Uchida<sup>1</sup>, Tatsuya Sano<sup>1</sup>, \*Hideki Mukoyoshi<sup>1</sup>

1. Department of Geoscience Interdisciplinary Graduate School of Science and Engineering, Shimane University

NW-SE trending small earthquakes swarm are observed along a zone of the center part of Shimane Prefecture to the northern part of Hiroshima Prefecture. Direction of the small earthquakes swarm is almost parallel to the aftershock distribution of the 2000 Western Tottori Earthquake (October 2000, M 7.3). The aftershock area of the 2000 Western Tottori Earthquake has experienced the M5 earthquake 8 times from 1950 until the main shock. In a similar fashion, small earthquakes swarm zone from the Sanbe-Miyoshi swarm earthquake zone has also experienced the M5 earthquake 12 times from 1950 until present day.

These similarity implies existence of concealed active faults along the Sanbe-Miyoshi swarm earthquake zone. Although previous studies in the aftershock area of the 2000 Western Tottori Earthquake revealed development of more than 1000 NW trending faults, the Sanbe-Miyoshi swarm earthquake zone has never been studied.

The purpose of this study is to understand the fault distribution and clarify their features in the southern part of the Sanbe-Miyoshi swarm earthquake zone.

The study area is a 6 km square around Kimita town in Hiroshima Prefecture. The investigation method is to record the fault by field survey and make thin section from sampled fault rock and observed the microstructure.

In the study area, Cretaceous rhyolite-dacite tuff and granite-porphry, Paleogene biotite granite and granite-porphry and Neogene Bihoku group (mudstone, sandstone, conglomerate) is exposed.

Total of 366 faults were observed in the study area. The orientation of these faults were concentrated in the about N56°W trend and inclined at a high angle to the north and south direction. In addition, strike of the fault was concentrated in the Northeastern part of the study area about N60°W, and in the Southwestern part about N20°W. The fault rocks in the northeastern part of the study area were hardly consolidated, but most of those of southwestern part were unconsolidated. The cutting relation of the fault was confirmed in the northeastern part of the study area. The fault of the NE trend was often cut the fault of NW trend.

In the southwestern part of the study area, fresh fault gouge was observed in a NW trending fault. Cutting relationship of the faults in this area were hardly observed.

This fresh fault is specific to the NW trending fault in the southwestern part, and unidentified in the NE trending fault.

Occurrence of fault rock in this study area implies that the fault system in the northeastern part is older than the those of southwestern part because consolidated fault rocks is commonly formed at the deeper part than the fault gouge. Cutting relationship of the faults in the northeastern part of the study area indicates NE trending fault is developed later than the NW trending fault. In the southwestern part of the study area, fresh fault gouge was observed only in the NW trending fault implies the NW trending fault is formed later than the NE trending faults.

Orientation of faults in this study area was concentrated at about N 56°W. But the distribution direction of small earthquake swarm in this study area is concentrated on about N40°W. Deviation of orientation of faults and distribution aftershock is reported at the aftershock area of the Western Tottori Earthquake and the deviated faults is thought to be Riedel shear planes of Early stages of fault development. However, the trend of faults and fault rocks in this study area is slightly different from the aftershock area of the Western

Tottori Earthquake. For example, most fault rocks in the northeastern part of the study area were consolidated (Most of the fault rocks in aftershock area of the Western Tottori Earthquake were unconsolidated ), and the faults in the southwestern part are concentrated in N20°W. From this fact, this study is thought to be faults related to aftershock distribution different from the study of previous research.

Keywords: microearthquake swarm, Sanin shear zone

# Distribution and characters of faults in the eastern Nanbu town and Houki town, Tottori Prefecture, western Japan

\*Tatsuya Sano<sup>1</sup>, Hideto Uchida<sup>1</sup>, Masaki Oku<sup>1</sup>, Takeshi Nagira, Hideki Mukoyoshi<sup>1</sup>

1. Department of Geoscience Interdisciplinary Graduate School of Science and Engineering, Shimane University

The 2000 Western Tottori earthquake occurred in a place where no clear active fault was identified because fault system in this area is presumably younger than another active faults. Previous study revealed development of more than 1000 WNW-ESE and NE-SW trending faults with very thin fault gouge in the aftershock area and adjacent outer area of the 2000 Western Tottori earthquake. However similarity and difference of distribution and characteristics of faults between in the aftershock area and the outside area was not well understood.

The objective of this study is to reveal the distribution and characters of faults which developed outside of the aftershock area of the 2000 Western Tottori earthquake by field survey and detailed observation of outcrop of faults and thin section.

This study area is located in the eastern Nanbu town and Houki town, Tottori Prefecture, which is located eastern outside of the aftershock area of the 2000 Western Tottori earthquake. In this area, the Late Cretaceous to Paleogene granitic rocks called the Neu Grenitic Pulton is widely exposed. The granitic rocks mainly consist of coarse-grained biotite granites and aplitic-pegmatitic granites. The western part and northeastern part of this study area, porphyritic biotite granites, and Pliocene olivine basalts and Pleistocene river terrace sedimentary layer is exposed respectively. Basalt-andesite dikes, rhyolite dikes, and aplite is intruded into the granitic rocks.

Fault orientation is generally concentrated in the N84°E82°N and N45°W77°N at the western area, N66°E78°N, N88°E90° and N70°W88°N at the central area, N68°W88°N at the east central area and N32°W86°N at the eastern area. Numerous whitish fault gouge were observed at the western and center area and most of faults in the east central area contains pinkish fault gouge. Thick damaged granite zone is also observed at the western area. The damage zone consists of hydrothermally altered cataclasite matrix with clasts of host rocks which are oriented in a certain direction. The damage zone have been formed by development of NE trending faults. Thickness of these NE trending fault is less than 1cm. Some NW trending faults with 2cm thick cut the NE trending faults. Arrangement of NE trending fault in center area is also observed.

Fault orientation in western and central part of this study area is similar with those of aftershock area and fault orientation in eastern part of area is similar with Komachi-Ohdani lineament. Color of fault gouge in western and central part of this study area is similar with those of aftershock area of 2000 Westrtn Tottori earthquake. In contrast, those of eastern part of area is similar with color of out of aftershock area which is revealed previous study. Therefore, fault system in western and central part of this study area is related to fault system in aftershock area. Fault system in eastern part of area related to Komachi-Ohdani lineament. Fault system in the 2000 Western Tottori earthquake expand 7km from epicenter in cross aftershock distribution. Western and central part of area may affected by the "Sanin shear zone".

Keywords: 2000 Western Tottori earthquake

## Fault zone development in the aftershock area of the 2016 Kumamoto earthquake, Kyushu, Japan

\*Kenta Kobayashi<sup>1</sup>, Keita Takahashi<sup>2</sup>, Shun Suzuki<sup>2</sup>, Ohashi Kenji<sup>1</sup>, Takuma Katori<sup>2</sup>, Minami Madoka<sup>1</sup>, Shuhei Tsukui<sup>1</sup>, Akari Imura<sup>1</sup>, Yuto Kato<sup>1</sup>, Naoki Takahashi<sup>1</sup>

1. Department of Geology, Faculty of Science, Niigata University, 2. Graduate School of Science and Technology, Niigata University

The Futagawa and the Hinagu fault zones were activated at the time of the 2016 Kumamoto earthquake. To understand how fault zones have developed over a long period of time, it is necessary to observe fault zone structures at the macro to microscope scales. We carried out field surveys in the NE-SW trending aftershock area of the earthquake, and analyzed the development of fractures, slip senses, and mineral assemblages at the fault zone.

The main shock (Mw7.0, April 16) occurred along the ENE-WSW trending Futagawa fault. On the other hand, the foreshocks (Mw6.2, April 14; Mw6.0, April 15) occurred along the NE-SW trending Hinagu fault. After the earthquake, many NE-SW~ENE-WSW trending surface ruptures were found along the Hinagu fault. They indicated dextral slip sense. In addition, a bed composed of lower terrace deposits was folded at the north end of the Hinagu fault. The fold hinge was plunging to NE.

Brittle fault rock zones were distributed in the Higo metamorphic rocks (Permian-Triassic). Andesite dikes (Neogene?) were intruded, also deformed along the faults. Most fault planes with NNW~NNE strike, indicated dextral, sinistral, normal and reverse slip senses. XRD analysis showed that the foliated cataclasite derived from pelitic-psammitic gneiss is mainly composed of smectite, kaolinite, chlorite and laumontite. The foliated gouges are abundant in smectite, contain chlorite and laumontite. NE-SW striking remarkable brittle shear zone was also recognized in the Hinagu Formation (Early Cretaceous), indicated dextral slip sense.

Viewed from the kinematics and the alteration process, the macroscale fault zone in the aftershock area has a long history of deformations. Parts of them were selected, and activated at the time of the 2016 Kumamoto earthquake.

Keywords: Kumamoto Prefecture, Hinagu fault, active fault, fault rocks



# Stress tensor inversion by using mixture probability distribution: Application to Quaternary meso-scale faults in Beppu area, southwest Japan

\*Katsushi Sato<sup>1</sup>

1. Division of Earth and Planetary Sciences, Graduate School of Science, Kyoto University

Stress tensor inversion techniques from orientations of faults is widely used in structural geology and seismology. Among them, the Hough method (Yamaji et al., 2006) has two advantages. One is to detect multiple stress states from a set of fault-slip data. The other is that incomplete fault-slip data which lacks information on slip orientations or shear senses can be utilized to constrain the stress states (Sato, 2006). However, the detection of optimal stress solutions has not been fully automated and there remains subjectivity in the result. This study aims at automating the detection of stress tensors.

The input data for stress tensor inversion is called fault-slip datum which carries fault plane orientation and slip direction. A reduced stress tensor, which has four degrees of freedom to be determined in the inversion analysis, corresponds to a point on five-dimensional (5-D) unit sphere (Sato and Yamaji, 2006). Assuming that a fault slips along the shear stress acting on the fault plane, a fault-slip datum constrains stress tensor to the corresponding points on a great semicircle on the 5-D unit sphere. The Hough method superimposes the semicircles specified by observed faults to obtain the distribution of objective function to be maximized. The peaks of the distribution give optimal reduced stress tensors. This study proposes to fit a mixture probability distribution to the distribution of objective function. The 5-D Kent distribution is employed as the component distribution in order to express the anisotropy caused by the shapes and the orientations of the great semicircles. The number of peaks is determined according to the Bayesian information criterion.

The new method was tested by the analysis of a synthetic fault-slip dataset, which consists of two groups of faults originated from different stress tensors. As the result, two given stress tensors are successfully detected. The new method was applied to meso-scale fault-slip data gathered from the Pleistocene Sekinan Group, Beppu area, southwest Japan. Two stress tensors were detected with NNE-SSW and NNW-SSE horizontal tension axes. Meso-scale faults cutting the Pleistocene Oita Group which overlies the Sekinan Group were also analyzed and only the NNE-SSW tensional stress was detected. These facts suggest that the tension orientation changed between 2.5 Ma and 1 Ma. The 68% confidence region of stress axes were also estimated by the bootstrap technique to be around 30 degrees.

## References

Sato, 2006, *Tectonophysics*, 421, 319-330.

Sato, K. and Yamaji, A., 2006, *Journal of Structural Geology*, 2006, 28, 957-971.

Yamaji, A., Otsubo, M. and Sato, K., 2006, *Journal of Structural Geology*, 28, 980-990.

Keywords: stress tensor inversion, fault-slip analysis, mixture probability distribution

# Spatiotemporal distribution of regional stress field associated with the 2016 Mw 7.8 Kaikoura earthquake estimated by stress tensor inversion of focal mechanisms in the northern South Island, New Zealand

\*Tadashi Sato<sup>1</sup>, Tomomi Okada<sup>1</sup>, Yoshihisa Iio<sup>2</sup>, Satoshi Matsumoto<sup>3</sup>, Stephen C Bannister<sup>4</sup>, John Ristau<sup>4</sup>, Shiro Ohmi<sup>2,5</sup>, Tsutomu Miura<sup>2</sup>, Jarg Pettinga<sup>6</sup>, Francesca Ghisetti<sup>7</sup>, Richard Sibson<sup>8</sup>

1. Research Center for Prediction of Earthquakes and Volcanic Eruptions, Graduate School of Science, Tohoku University, Japan, 2. Disaster Prevention Research Institute, Kyoto University, Japan, 3. Institute of Seismology and Volcanology, Faculty of Sciences, Kyushu University, Japan, 4. GNS Science, New Zealand, 5. Earthquake Hazards Division, Disaster Prevention Research Institute, Kyoto University, Japan, 6. University of Canterbury, New Zealand, 7. Terra Geologica, New Zealand, 8. University of Otago, New Zealand

The northern South Island and the southernmost North Island of New Zealand occupy the transition region between subduction and transform tectonics along the Pacific-Australia plate boundary, with the Pacific plate subducting beneath the Australian plate obliquely from the northeast. Active seismicity in the northern South Island results from a combination of subduction and transform tectonics. An Mw 7.8 earthquake involving a combination of reverse and mostly dextral strike-slip faulting occurred in the Kaikoura region of northern South Island at 11:02.56 am (UT) on 14 November 2016. In this study, we estimated the spatio-temporal variation of the crustal stress field by stress tensor inversion using focal mechanisms obtained from micro- to moderate-sized earthquakes.

We analyzed the data acquired by a dense seismic array which has been recording over 2 years from 1 April 2013 to April 2015. We determined focal mechanisms using the HASH program (Hardebeck, 2002; 2003) and estimated the spatio-temporal variation of the crustal stress field using SATSI algorithm (Hardebeck and Michael, 2006). During that time period, there were two major seismic clusters; the first, consisting of aftershocks of the 1990 Lake Tennyson earthquake, occurred in the center of the northern South Island, while the second, consisting of aftershocks of the 2013 Cook Strait earthquakes, occurred in the northeast of the northern South Island. For shallow earthquakes, strike-slip type focal mechanisms were dominant. P axes were oriented ~N120E, similar to that found in previous studies (Reyners et al., 1997; Balfour et al., 2005; Sibson et al., 2011; Townend et al., 2012). T axes were oriented NE-SW. For intermediate-deep earthquake, normal, strike-slip, and reverse faulting seems to be mixed. Most of the P axes were oriented NE-SW, which is also consistent with previous studies (Reyners et al., 1997; Townend et al., 2012).

Next, we conducted stress tensor inversion using SATSI algorithm by dividing the earthquakes into three groups; 0-27km depth, 27-40km depth and deeper than 40km. On the 0-27km depth, the  $\sigma_1$  axis was oriented ~N120E with high accuracy, while for earthquakes deeper than 40km, the  $\sigma_1$  axis was oriented ~N60E with high accuracy. Therefore the shallow crustal stress orientation differed from the deep orientation which corresponds to the condition within the subducting Pacific plate.

For the 2016 Kaikoura earthquake, we also used the GeoNet CMTs in the period of approximately three months from 14 November 2016 to 31 January 2017 to estimate the regional postseismic stress field using the SATSI algorithm. The GeoNet CMTs show, that most of the events were shallower than 30 km, with event depths increasing northeast from the mainshock hypocenter. There have been almost three major clusters: the first (the C cluster) is almost in the center of the aftershock area, the second (the NE cluster) is northeastern margin of the aftershock area, and the third (the SW cluster) is around the main shock hypocenter. P axes were oriented to E-W in the NE cluster, while oriented to N120E in the C and

SW clusters. T axes were oriented to N-S in the NE cluster and oriented to NE-SW in the C and SW clusters.

We conducted stress tensor inversion using the SATSI algorithm for the events in the 0-27km depth. The  $\sigma_1$  axis was oriented E-W in the NE cluster while  $\sigma_1$  axes were oriented N120E in the C and SW clusters. We compare the stress tensor solutions before and after the Kaikoura earthquake. The orientations of  $\sigma_1$  axes are similar, but the 95 % confidence range became wider. This reflects a decrease in the magnitude of  $\sigma_1$  because of the earthquake, with it becoming closer to the magnitude of  $\sigma_2$ .

Keywords: Northern south Island of New Zealand, Regional stress field, 2016 Mw 7.8 Kaikoura earthquake, Stress tensor inversion

# Fault evolution process related to stress field transition around the Byobuyama fault, central Japan

\*Takuma Katori<sup>1</sup>, Kenta Kobayashi<sup>1</sup>

1. Graduate School of Science & Technology, Niigata University

The central Japan is one of the concentrated area of active faults, which consist of the complicated fault geometry system. It has been reported that the origin of such fault zones can be traced back to the formation of cataclasite zone in late Cretaceous to early Paleogene (Oohashi and Kobayashi, 2008; Niwa et al., 2011). But, the fault development history reported in previous researches has lower resolution than the plate motion history, especially in Neogene period. Therefore, we performed structural study focused on the Byobuyama fault, central Japan. The Byobuyama fault is suitable for constraining the age of fault movement because Miocene Mizunami group and Pliocene-Pleistocene Toki Sand and Gravel formation are located around the fault. To reconstruct the history of the fault movement, we performed a detailed investigation along the Byobuyama fault and collected samples for structural and chemical analyses. To understand structural history, paleo-stress fields analysis using the Multiple Inverse Method (Yamaji, 2000) were performed. Chemical analysis with XRD, XGT, SEM-EDS and EPMA-WDS analyses also conducted. Based on these analyses, following results were obtained.

## < Stress Fields >

Comparing the data of cross-cutting relationship with the result of paleo-stress analysis, the following transition history details were obtained. Cataclasite formation under WNW-ESE trending compression, vertical trending extension (Stress A) → Fault gouge formation under NNE-SSW trending compression, vertical trending extension (Stress B) → Fault gouge formation under ENE-WSW trending compression, NNW-SSE trending extension (Stress C) → Fault gouge formation under WSW-ESE trending compression, NNE-SSW trending extension (Stress D).

## < Deformation and Alteration >

The cataclasites which received stronger deformation were formed at the later stage. Proto cataclasite is composed stilbite vein and ortho cataclasite composed calcite vein. The matrix of the Stress B gouge is composed mainly of illite. In contrast, smectite is abundant in the Stress C and D gouges.

From the above results, it is evident that the Byobuyama fault has experienced tectonic activities of several stages under different stress states, and significant differences in the deformation and alteration mechanisms exist between these stages. It is considered that the timing of the cataclasite formation correspond to Eocene because Stress A condition matches the convergence direction of the Pacific plate at the time (Maruyama et al., 1997). In previous studies within the Tsukiyoshi fault which adjacent to the Byobuyama fault, a reverse fault movement was detected during deposition of the Mizunami group under N-S compression (Khoriya et al., 2003). It is observed that Stress B also corresponds to this event and related to the collision of Izu-Bonin arc (Tsunakawa, 1986). Since Toki sand and gravel formation not experienced Stress C deformation, it is speculated that this event occurred around Pliocene. Finally, it is identified that Stress D correspond to an active fault event because 1) Toki sand and gravel formation encounter the deformation, 2) Stress D state is consistent with the current stress field. These results with high-resolution tectonic history is considered to be an important achievement on constructing structural evolution history of central Japan.

## Reference

Oohashi, K. and Kobayashi, K., 2008, Jour. Geol. Soc. Japan, 114, 16-30.  
Niwa, M. et al., 2011, Engineering Geology, 119, 31-50.

Yamaji, A., 2000, *Jour. Stru. Geol*, 22, 441-452.

Maruyama, S. et al., 1997, *The Island Arc*, 6, 121-142.

Khoriya, Y. et al., 2003, *JpGU Meeting 2013 G015-P003*.

Tsunakawa, H., 1986, *Jour. Geomag. Geoelectr.*, 38, 537-543.

Keywords: Fault evolution, Stress field, Active fault, Byobuyama fault

# Generation of pseudotachylyte and interseismic plastic deformation in ancient crustal seismogenic fault zones, Yawatahama-Oshima, Ehime, Japan

\*Aiu Ono<sup>1</sup>, Tsuyoshi Toyoshima<sup>2</sup>, Masayuki Komatsu

1. Graduate School of Science and Technology, 2. Department of Geology, Faculty of Science, Niigata University

Three pseudotachylyte-producing fault zones develop in Yawatahama-Oshima, Ehime, Japan (Komatsu et al., 1997, 1998). The Yawatahama-Oshima pseudotachylytes and their related fault rocks were formed under greenschist-facies conditions (upper continental crustal conditions) (Komatsu et al., 1997, 1998; Komatsu, 2001). We illustrate generation of the Yawatahama-Oshima pseudotachylyte accompanied by plastic deformation, as an example of ancient seismogenic fault zones in upper crust.

Pressure solution-precipitation structures (pressure solution cleavage accompanied by quartz and feldspar veins) are characteristically abundant in the Yawatahama-Oshima pseudotachylyte-producing fault zones. Modes of occurrence of the Yawatahama-Oshima pseudotachylytes and pressure solution cleavage indicate that seismic slip with pseudotachylyte generation and slow plastic deformation (pressure solution with precipitation) alternated in the same fault zones and along the same fault surfaces. Therefore we can conclude that pressure solution-precipitation is likely one of the principal deformation mechanisms for interseismic plastic deformation and time-dependent strength recovery of the Yawatahama-Oshima pseudotachylyte-producing fault zones. Their strength recovery processes are explained by a solution-precipitation model, which was proposed for the Hidaka pseudotachylytes from the Hidaka metamorphic belt, Hokkaido, by Wada and Toyoshima (2007).

Keywords: pseudotachylyte, plastic deformation, pressure solution cleavage

# Interseismic plastic deformation in paleo-seismic fault zones under lower crustal conditions at Tonagh Island in the Napier Complex, East Antarctica

\*Tsuyoshi Toyoshima<sup>1</sup>, Norio Shigematsu<sup>2</sup>, Yasuhito Osanai<sup>3</sup>, Masaaki Owada<sup>4</sup>, Toshiaki Tsunogae<sup>5</sup>, Tomokazu Hokada<sup>6</sup>

1. Department of Geology, Faculty of Science, Niigata University, 2. Research Institute of Earthquake and Volcano Geology, Geological Survey of Japan, National Institute of Advanced Industrial Science and Technology, 3. Division of Evolution of Earth Environments, Faculty of Social and Cultural Studies, Kyushu University, 4. Graduate School of Science and Engineering for Innovation, Yamaguchi University, 5. Faculty of Life and Environmental Sciences (Earth Evolution Sciences), University of Tsukuba, 6. National Institute of Polar Research

There are several; granulite-facies paleo-seismic fault zones (PSF) in Tonagh Island, the Napier Complex, East Antarctica (Toyoshima et al., 1999, 2016). In PSF, alternation of thin ultramylonites, cataclasites, pseudotachylytes, and mylonitized pseudotachylytes occur, showing that multiple generations of pseudotachylytes, cataclasites and ultramylonites.

Two types of granulite-facies ultramylonites occur in PSF: type 1 and 2. Microstructures of recrystallized plagioclase and quartz suggest high-temperature or low-strain rate crystal plastic deformation. Microstructures of recrystallized quartz in type 2 ultramylonites suggest high-strain rate crystal plastic deformation. Z-maximum c-axis lattice preferred orientation (LPO) patterns for quartz in type 2 ultramylonites suggest a basal slip system dislocation creep and high-strain rate crystal plastic deformation during interseismic periods. There are two alternative possibilities of deformation mechanisms of quartz in type 2 ultramylonites as follows: (1) Mylonitized quartz layers originated from quartz veins parallel to mylonite foliation. (2) Water weakening occurred during mylonitization of quartz. Microstructures and LPO patterns of recrystallized plagioclase indicate switch in deformation mechanism from dislocation creep to grain-boundary sliding in type 2 ultramylonites, and also suggest that continuous low strain rate or low differential stress plastic deformation and seismic events alternated. This is imaged acceleration of strain rate or stress relaxation before or after seismic events, respectively. The switch in deformation mechanism from dislocation creep to grain-boundary sliding, associated with the grain-size reduction, attests of the mechanical softening during deformation, which contributed to the localization of the strain within the mylonite, as suggested by Raimbourg et al. (2008).

Keywords: pseudotachylyte, high-strain rate crystal plastic deformation, grain boundary sliding

# The role of fracturing in the formation of lower crustal shear zones

\*Takamoto Okudaira<sup>1</sup>

1. Department of Geosciences, Graduate School of Science, Osaka City University

Plagioclase-rich rocks are major constituents of the lower crust, and then understanding the rheological properties and deformation processes of plagioclase-rich rocks is key to evaluating the strength and mechanical behavior of the lower crust. Investigating grain size reduction and possible subsequent grain-size-sensitive (GSS) deformation in plagioclase-rich rocks is particularly important because a transition to GSS creep would result in significant rheological weakening. Dynamic recrystallization is a common grain-size reduction mechanism in plagioclase aggregates deformed by grain-size-insensitive (GSI) dislocation creep under conditions of the amphibolite to granulite facies. Empirical relationships between stress and recrystallized grain size have been proposed for plagioclase aggregates. If such stress and grain size relations transect the boundary between GSI and GSS creep fields, grain size reduction by dynamic recrystallization can lead to a transition from GSI dislocation creep to GSS creep. However, in the GSS creep field the applicability of the empirical piezometer is problematic owing to a potential lack of driving force for recrystallization. Dynamic recrystallization may represent a balance between grain size reduction and crystal growth processes set up in the boundary region between the GSI and GSS creep fields, and then recrystallized grain size and stress balance near the GSI-GSS field boundary. Thus, major weakening in localized natural deformation zones is unlikely to be caused by dynamic recrystallization. Fracturing and/or comminution are dominant grain-size reduction mechanisms at low temperatures because the critical resolved shear stress may not be reached in plagioclase, and recovery and recrystallization are limited. However, even under high-temperature conditions where plagioclase undergoes plastic deformation, fracturing and nucleation of new grains as small fragments has been identified in naturally and experimentally deformed rocks. Zones of very fine grains that result from fracturing and/or comminution would deform by GSS creep and then would develop as ductile shear zones in the lower crust. In this study, we summarized the  $P$ - $T$  conditions of dynamic recrystallization and fracturing in the lower crustal plagioclase-rich rocks, and will discuss the formation and development of shear zones in the lower crust.

Keywords: Rheology, Lower crust, Shear zone, Fracturing, Dynamic recrystallization, Plagioclase



# Importance of fault rheology around brittle-plastic transition in long-term behavior of major faults

\*Hiroyuki Noda<sup>1</sup>

1. Kyoto University, Disaster Prevention Research Institute

Fault behavior such as long-term slip rate, magnitude and recurrence interval of earthquakes, and reaction against stress perturbation depends on the loading condition and mechanical properties of the fault. In considering the latter factor, existence of a ductile shear zone, which underlies a seismogenic part of a major fault, may be of great importance; the brittle-plastic transitional regime has maximum shear resistance in a classical Christmas-tree strength profile, and the slip there directly load the shallower seismogenic part of the fault. In order investigate the long-term, time-averaged fault behavior, numerical simulations of earthquake sequences on a major fault with a ductile shear zone have been conducted in the present study in a simplified geometry.

An elastic crustal plate with a through-going strike-slip fault is assumed, and the fault motion is driven by applying constant far-field shear stress  $\tau_{pl}$ . A rate- and state-dependent friction-to-flow fault constitutive law [Shimamoto and Noda, 2014] is used in the present study. In this law, shear resistance is approximately given by a rate- and state-dependent friction law in a shallow brittle part of the fault, and by power-law creep of quartzite (exponent: 4) in a deep, fully plastic part. The rate-dependency of the shear resistance takes the maximum value in a transitional regime between them. Note that the peak in the rate-dependency does not necessarily correspond with peak shear resistance. If we assume excess pore pressure at depth which limits the effective normal stress at a certain value, then a Christmas-tree strength profile does not exist, but a remarkable peak in the rate-dependency still appears in the transitional regime.

In the simulations, the fault hosts repeating earthquakes in the brittle part, and slips by a long-term speed  $V_{pl}$  on average which depends on  $\tau_{pl}$ . The relation between  $\tau_{pl}$  and  $V_{pl}$  is very well explained by a power law with the exponent about 20. This is similar to what is followed by unstable steady-state solutions with uniform slip rates  $V_{ss}$ . It should be noted that  $V_{pl}$  is larger than  $V_{ss}$  for the same  $\tau_{pl}$  approximately by a factor of 2 as long as studied. This is because the brittle part of the fault typically support smaller shear stress than the steady-state level, and thus the ductile shear zone support larger shear stress associated with larger slip rate than the steady state. Since the relation between  $\tau_{pl}$  and  $V_{ss}$  is given by spatial average of the rate-dependency, the transitional regime having the prominent peak in the rate-dependency most significantly contributes to the amount of shear stress perturbation required to change the long-term slip rate of the fault. It should be emphasized that the brittle-plastic transitional regime is important not only because of the maximum strength potentially existing there, but also because of the maximum rate-dependency.

Keywords: Brittle-plastic transition, Earthquake sequence, Long-term fault motion

## Fracture contact state inferred from longitudinal wave velocity: Theoretical and experimental approach

\*Eranga Gayanath Jayawickrama<sup>1</sup>, Hayata Tamai<sup>2</sup>, Jun Muto<sup>1</sup>, Hiroyuki Nagahama<sup>1</sup>

1. Department of Earth Science, Tohoku University, 2. East Japan Railway Company

Seismic tomography has provided many important details of the earth's interior in the past few decades and variation in wave velocity has been a key factor in understanding the seismograms. Therefore, by velocity inversions the understanding of low velocity zones within the earth's crust has been improved and in general these low velocity zones are identified as zones with fluids or geologically weak zones. In reflection seismology, low velocities can be identified as weak zones, basically as fractures. Even though these inversions have the ability to show the fractured zones, they have not been able to show the degree of opening of the fractures. Therefore, to understand the fracture contact state, it is important to achieve a relationship between the contact state and the velocity, so that by the variation in velocity the contact state can be inferred.

As to the current knowledge, the elastic wave velocity is highly affected by the fractures, and this indicates that the contact state has a strong influence over the variation in velocity. The wave velocity increases as the contact state changes its relative displacement with increasing pressure. This change in displacement was explained by Nagumo (1963) for different types of single contacts. In this study, we have extended this pressure-displacement relationship of single contacts to a velocity-pressure relationship, and discuss the multiple contact state variation inferred from the change in velocity with increasing pressure.

From one dimensional wave equation, a power law relationship of longitudinal wave velocity and pressure is introduced with a pressure exponent representing the contact state of fractures. For single cone, ball and flat contacts, the pressure exponent  $\lambda$  takes values of 1/2, 1/3 and 0, respectively. By extending this to multiple contacts the pressure exponent  $\mu$  representing multiple contacts have been deduced as 2/3, 3/5 and 1/2 for multiple cone, ball and flat contacts, respectively. Using previously published experimental data and an empirically derived equation (Kobayashi and Furuzumi, 1972) which is similar to the theoretically derived relationship in the current study, the applicability of the theory is tested. From the results, we show that the contact state changes from conical contacts, to ball contacts and finally to flat contacts with increasing pressure.

The study has also shown that the lithology, microstructures and presence of water are factors that control the contact state with increasing pressure. Granite and gabbro show pressure exponents  $\mu < 1/2$  indicating complete closure of fractures while serpentinite is yet to close completely at the same pressure. Also, rocks with equally low porosity but different lithologies show different contact states at equal pressures. These indicate that lithology is a major factor controlling the contact state. Further a marked difference in contact states can be observed depending on the direction of measurement with respect to the foliation and depending on the water existence. The velocity change with increasing pressure also can be explained in terms of contact state of fractures using the current contact state theory since the prominent velocity change is mimicked by an equally prominent contact state change at the same pressure.

As shown from our study, this method is applicable to assess the contact state of fractures in an area of interest. By obtaining velocity data from reflection seismology and seismic tomography, and using the wave velocity-contact state relationship introduced here, the degree of fracture opening can be estimated. Therefore, we believe this method can be used in wide range of applications from shallow depth exploration geophysics to understanding the anomalies in lower crust.

Keywords: Contact state, Fractures, Wave velocity

# Microstructures and quartz c-axis fabrics in granitic protomylonite from the Median Tectonic Line fault zone, Mie Prefecture, south-west Japan

\*Dong Van Bui<sup>1</sup>, Toru Takeshita, Jun-ichi Ando, Takafumi Yamamoto

1. Department of Natural History Sciences, Graduate School of Science, Hokkaido University

During major orogenic events, the conditions and mechanisms of deformation play an important role in their development. Deformation conditions and histories can be obtained from various microstructures in constituting mineral phases of deformed rocks. Among them, quartz c-axis fabrics in quartz-rich tectonites are the very useful indicators. In this study, we will report microstructures and quartz c-axis fabrics from granitic protomylonite to mylonite, which occur along the Median Tectonic Line (MTL), Mie Prefecture, south-west Japan, and infer deformation conditions and histories during the development of the MTL. The MTL is a major strike slip fault system with the largest structural break in southwestern Japan that has been defined as the boundary fault between Sambagawa metamorphic rocks and Ryoke granitic and metamorphic rocks. Protomylonite in the MTL was derived from granitoids in the Ryoke belt in the latest Cretaceous called the Kashio phase, before the MTL was formed as the boundary fault during the exhumation of the Sambagawa metamorphic rocks at 63-58Ma (Kubota and Takeshita, 2008). Protomylonite from the MTL, which suffered cataclasis to a certain degree, consists of quartz ribbons and feldspar porphyroclasts in a matrix consisting of finely-crushed quartz and feldspar porphyroclasts, chloritized mafic minerals, muscovite altered from plagioclase, and calcite veins. The feldspar porphyroclasts show many extension fractures with  $\sigma_1$  being perpendicular to the foliation. Some of the feldspar porphyroclasts are decorated by recrystallized feldspar grains along grain boundaries. The quartz ribbons are large and strongly flattened relic grains showing undulatory extinction, deformation lamellae, and fluid inclusion arrays, surrounded by very-fine recrystallized quartz grains indicating bulging recrystallization (Stipp et al., 2002). Type III and type IV deformation twin of calcite (Burkhard, 1990) dominate in the calcite veins.

The c-axis orientation distribution of large quartz grains was measured by a scanning electron microscope (SEM; JEOL JSM6390A) equipped with an electron backscatter diffraction (EBSD) detector, which mostly shows a Y maximum with type II crossed girdles indicating dominant operation of prism {10-10} slip system and a type I crossed girdle pattern with r-maxima for a small number of samples indicating the dominant operation of rhomb {1011} slip (Tullis, 1977; Lister and Hobbs, 1980; Schmid and Casey, 1986; Law, 1990; Heilbronner and Tullis, 2002; Takeshita et al. 1999; Okudaira et al. 1995).

The crystallographic orientation map of recrystallized quartz grain, which was measured by the EBSD mapping with step size of 1 micrometer, illustrated many subgrain boundaries and small recrystallized grains surrounded by larger recrystallized grains, suggesting a strong overprinting recrystallization at higher differential stresses. Two groups of recrystallized quartz grain occur in the protomylonite samples: the larger and the smaller recrystallized quartz grains with the size of approximately 70 micrometer and 10 micrometer, respectively. Further, several sizes of dynamically recrystallized fine-grained quartz are observed at the peaks of approximately 20 micrometer and 45 micrometer.

The Y-max quartz c-axis fabric associated with the coarse-grained recrystallized quartz (70 micrometer) could indicate the deformation temperatures in protomylonite samples around intermediate temperatures (400-500 °C), whereas the fine-grained recrystallized quartz (10 micrometer) could have formed at temperatures of 300-400 °C based on the paleostress estimation from recrystallized quartz grain size (e.g. Stipp and Tullis, 2003) and constitutive equations of flow in quartz aggregates (e.g.

Gleason and Tullis, 1995). Thus, overprinting deformation could have occurred in these protomylonites along the MTL, represented by the reduction of recrystallized quartz grain size from c. 70 micrometer to c. 10 micrometer with several peak sizes of dynamically recrystallized fine-grained quartz. This overprinting deformation could have occurred heterogeneously in both spatial and temporal development during the exhumation of protomylonite along the MTL.

Keywords: Microstructures, Quartz c-axis fabrics , Protomylonite, The MTL

## Frictional properties of the Median Tectonic Line fault zone

\*Miki Takahashi<sup>1</sup>, Chisaki Inaoi<sup>2</sup>, Jun Kameda<sup>3</sup>, Norio Shigematsu<sup>1</sup>

1. Institute of Earthquake and Volcano Geology, Geological Survey of Japan, AIST, 2. Department of Natural History Sciences, Graduate School of Science, Hokkaido University, 3. Earth and Planetary System Science Department of Natural History Sciences, Graduate School of Science, Hokkaido University

We investigated frictional properties of fault gouges of the Median Tectonic Line (MTL) at an outcrop (Awano-Tabiki outcrop) exposed in the eastern Kii Peninsula, Japan, using a laboratory experiment technique to evaluate a strength-history of the MTL fault. Shigematsu et al., (2017) described that the MTL fault zone at Awano-Tabiki outcrop is suffered four stages of faulting under different depths in brittle regime. The newest deformation at the Awano-Tabiki outcrop (stage 4) is characterized by a localized zone with a normal faulting sense of slip within  $\sim 1$  cm in thickness (gouges-B and F). Those gouges are rich in smectite, indicating that the depth to activate the MTL fault at this stage would be relatively shallow at which the temperature is lower than 140 deg.C. On the other hand, the oldest deformation (stage 1) is widely distributed in such as gouges D, I-L with a dextral sense of slip. They are rich in muscovite and illite, indicating that corresponding temperature could be higher than 200 deg.C. Therefore to investigate frictional property of each fault gouge at each deformation condition based on mineral compositions, could be a key to reveal a history of a crustal fault strength such as the MTL fault. An experimental machine we used was a gas-medium, high-pressure, high-temperature triaxial apparatus set at GSJ, AIST, Japan. We set initially temperature conditions,  $T$ , to 100 deg.C for gouge-B and gouge-F and to 250 deg.C for gouge-D, respectively. Then, confining pressures,  $P_c$ , corresponding to assumed depth were determined by assumed geothermal gradient (20~60 deg.C/km). We thought conditions of pore pressure,  $P_p$ , and sliding velocity,  $V$ , would change in the earthquake cycle. We, therefore, varied the values of  $P_p$  (hydrostatic  $\sim P_c$ ) and  $V$  (0.011 mm/sec  $\sim$  115 mm/sec for stepwise change). After 75 mm mesh sieving, 0.6 g of smaller-grain-sized powder sample of the gouge was sandwiched between porous alumina pre-cut blocks, which provided c.a. 0.5 mm thick gouge layer. The powder samples of gouge-B and gouge-F contained 24 wt.% and 34 wt.% of smectite, respectively. On the other hand, the powder sample of gouge-D was rich in muscovite (26 wt.%) and illite (21 wt.%), but did not contain the smectite. We obtained interesting results on both the shear strength and the velocity dependence of friction for those smectite rich gouges. Average values of friction coefficient, showing a dependence of the smectite content, are 0.30 for gouge-B and 0.18 for gouge-F. However, the friction coefficient for both gouges became decreasing significantly towards  $\sim 0.05$  at  $P_c - P_p <$  c.a. 14 MPa, while the frictional coefficient on gouge-D showed a constant value of 0.42 with no effective pressure dependence. Common properties of the gouges were that the velocity dependence of friction became positive at high  $V$ , low  $P_p$  and high smectite content but became negative at the low  $V$ , high  $P_p$  and low smectite content. We will, thus, add cases for other samples of gouge zones formed between oldest stage generating gouge-D and newest stage generating gouge-B and -F to complete a figure for the strength-history of the MTL fault.

Keywords: fault gouge, the Median Tectonic Line fault, velocity dependence of the friction, friction coefficient

# Study of rheology and origin of deformed conglomerates, Pliocene Hamaishidake Formation Fujikawa Group, Eastern part of Shizuoka prefecture, Central Japan -Tectonics of the collision zone recorded deformed conglomerate-

\*Shun Suzuki<sup>1</sup>, Kenta Kobayashi<sup>1</sup>

1. Graduate School of Science & Technology, Niigata University

South Fossa Magna is located at the meeting part of the Philippine Sea, Eurasia, North America Plate, and it is the most variable zone in Japan. It has also attracted attention as a multiple collision and addition site for the Honshu arc of the Izu-Ogasawara arc on the Philippine Sea Plate. Hamaishidake Formation of Fujikawa Group (Upper Miocene-Pliocene) widely distributed in this study area is trench-fill sediments in connection with collision event, which consists of conglomerate and volcanic clastic rock. The Fujikawa estuary fault zone (Iriyama and Shibakawa fault, total length is over 26km) runs NS trend between the Hamaishidake Formation on the west side and the Ihara Group (Pleistocene) on the east side. And it is said that the southern extension of these fault zone connects to Suruga trough (Sugiyama and Shimokawa, 1982). Therefore, it is expected that the trench-fill sediments is recorded traces of complex tectonics at the plate boundary. Furthermore in recent years, outcrop of foliated cataclasite which undergoes brittle deformation while flowing was reported in the conglomerate layer of the Hamaishidake Formation (Maruyama, 2008). Its continuity and the cause remain unknown because foliated cataclasite has not been known from Hamaishidake Formation so far. So in this study, in order to elucidate the tectonics in the collision zone, we carried out basic description of foliated cataclasite outcrop and various analyses based on them.

Foliated cataclasite (Fuji River shear zone) is exposed to the riverbed near the Shin-Uchibusa bridge over the Fuji River, southwest part of Fujinomiya City, Shizuoka Prefecture. (Outcrop size is 30m E-W, 300m N-S). Deformation is not uniform, we confirmed some deformation convergence zone. Strike of the formation and trend of the shear zone are almost parallel. These basic trends are N45°-60°W, but EW trend is also confirmed. The deformation style of the gravel is diversified from non-deformation type to developed shear type, and gravel which the outer shape flows type (Cataclastic flow), and there are confirmed coexisting. The shear sense required from the fabric of gravel shows sinistral sense. The continuity of the shear zone was not recognized in this survey. In the surrounding geology, it was found that brittle deformation accompanying the NS folding structure and fault gouge is dominant. In addition, we measured structure of the fault plane at various places, and determined old stress by using multiple inverse method (Yamaji, 2000 etc.). As a result, we got lateral fault stress field of NNE-SSW  $\sigma_1$  from the Fujikawa shear zone, reverse fault stress field of EW  $\sigma_1$  from the surrounding fault gouge, and sinistral fault field of WNW-ESE  $\sigma_1$  from the fracture zone near the Iriyama fault.

Results of such description and analysis, It became clear that the shear zone has a local distribution which has a basic structure (NW-SE trend) obliquing with the surrounding geological structure (NS trend). And considering the resume depth of the fault rock, there is a clear gap in the deformation style between the shear zone and its surrounding geology. If the shear zone is formed deeper depth than the fault gouge forming resume depth, it is conceivable that there was a local geological rising event after the folding because NW-SE trend structure of the shear zone cuts the fold structure of the surrounding NS system. From the stress analysis result, first works in this study area, The lateral shear stress field of NNE-SSW

compression, which forms the shear zone. Along with the rise of the geologic body, they converted into EW compression which contributed to the formation of NS fold structure system. And NS fault system acted as reverse fault. After that, Iriyama fault started sinistral sense under the WNW-ESE compression stress field. In this presentation, we will discuss the history of geological structure development at the plate boundary from such descriptions and analysis results.

Keywords: South Fossa Magna, multiple collision zone, Fujikawa estuary fault zone, deformed conglomerate, fault rocks



## sintering polycrystalline olivine from pulverized olivine crystals

\*Yumiko Tsubokawa<sup>1</sup>, Masahiro Ishikawa<sup>1</sup>

1. Faculty of Environment and Information Sciences, Yokohama National University

The rheological properties of Earth's interior have been determined by laboratory experiments of polycrystalline samples of rock-forming minerals. In these deformation experiments, fine-grained specimens are often required for deformation in diffusion creep regime at laboratory strain rates (e.g. Karato, 2010). In this study, we successfully fabricated olivine nano-sized powder from naturally occurring olivine single crystal (peridot:  $\text{Mg}_{1.76-1.84}\text{Fe}_{0.16-0.24}\text{SiO}_4$ ). In order to investigate a method for preparing fine-grained and highly dense nanocrystalline olivine, the sintering behavior of olivine powder was studied. Olivine powder were pressed into cylindrical shape and sintered under argon flow at temperatures ranging from 1130-1350 °C for 2-6 hours. After the sintering, sample surfaces were polished and thermally etched to expose grain boundaries. Grain size and porosity were determined from the microstructure of scanning electron microscope. Olivine grains in sintered samples are polygonal and isotropic shape, and show a homogeneous structure. The average grain size increased with increasing sintering time and sintering temperature, and a significant grain growth was found for the sample sintered at 1350 °C. At temperatures of 1300 °C, we could obtain dense polycrystalline olivine with an average grain size of  $< 2 \mu\text{m}$ .

Keywords: sintering, olivine, polycrystalline

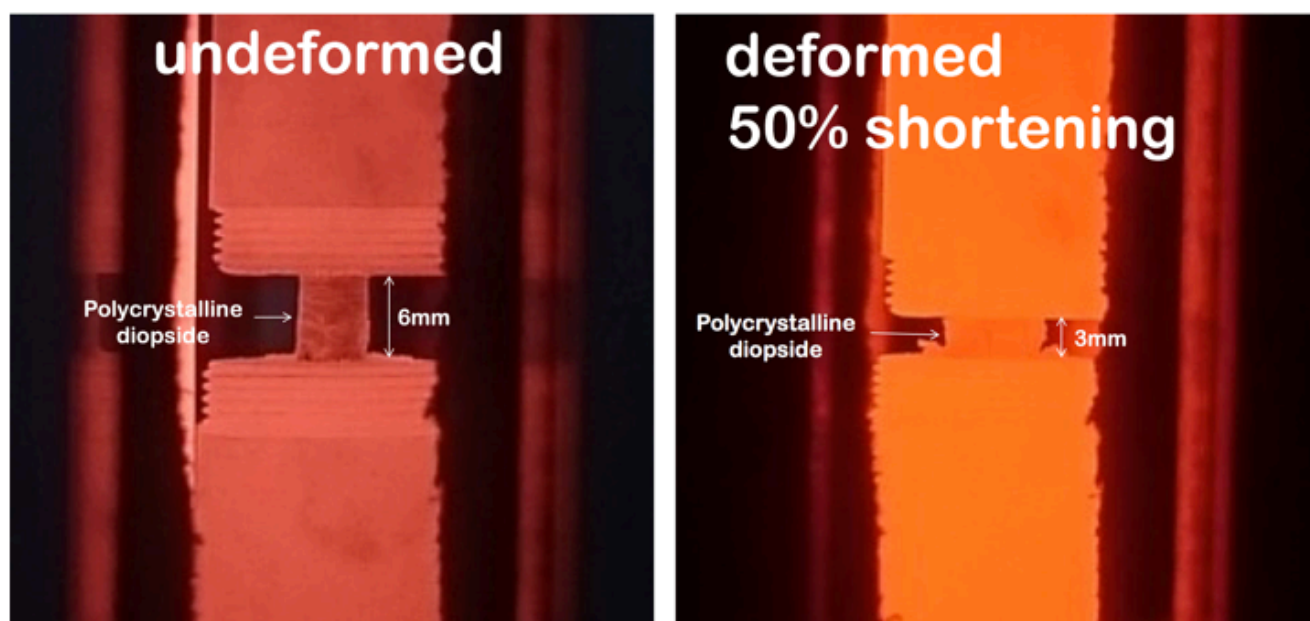
## Viscosity and graphitic carbon weakening of diopside

\*Masahiro Ishikawa<sup>1</sup>, Yumiko Tsubokawa<sup>1</sup>

1. Graduate School of Environment and Information Sciences Yokohama National University

Dynamic behaviours of Earth's plates are strongly dependent on the viscosity of Earth's upper mantle. Although a trace amount of hydrogen can markedly weaken the upper mantle, the influence of carbon on viscosity of the upper mantle is unknown. Here we report the deformation experiment of diopside, one of the main constituents of the upper mantle. In order to investigate influence of graphite on creep properties of diopside, we prepared graphite-bearing nano-polycrystalline diopside (average grain size  $\phi = 0.4 \mu\text{m}$ ). Deformation experiments have been carried out on graphite-bearing nano-polycrystalline diopside in argon gas atmosphere in a uniaxial deformation apparatus. A homogeneous shortening was observed when the graphite-bearing nano-polycrystalline diopside specimen was compressed at 1080 °C and 1060 °C under subsolidus conditions. The stress exponent  $n=1.08$  at 1080 °C suggests that the deformation mechanism of the graphite-bearing nano-polycrystalline diopside is dominated by diffusion creep rather than dislocation creep. Viscosity of the graphite-bearing nano-polycrystalline diopside ( $1.00\text{-}1.25 \times 10^{11}$  Pa s at 1080 °C) is much lower than that of graphite-free diopside aggregates. Our results demonstrate that diopside is weakened by a small amount of graphite.

Keywords: diopside, graphite, carbon, viscosity, sinter, nano



## Fabrication of albite aggregate by hot pressing

\*Norio Shigematsu<sup>1</sup>, You Zhou<sup>2</sup>, Hideki Hyuga<sup>2</sup>, Yuichi Yoshizawa<sup>2</sup>

1. Research Institute of Earthquake and Volcano Geology, Geological Survey of Japan, National Institute of Advanced Industrial Science and Technology, 2. Structural Materials Research Institute, National Institute of Advanced Industrial Science and Technology

Feldspar is one of the main constituent minerals of the Earth's crust. The mechanical behavior of plastic deformation of feldspar has previously well studied especially for anorthite ( $\text{CaAl}_2\text{Si}_2\text{O}_8$ ), because this controls the strength of the lower crust. On the other hand, several studies of natural fault rocks and experimental results suggest that plagioclase with composition close to albite ( $\text{NaAlSi}_3\text{O}_8$ ) shows complicated transient behaviors of plastic deformation which possibly control the shear localization and the nucleation of fractures in the crust. In this study, we examined a method to fabricate aggregate of albite to examine such properties experimentally in future.

Albite powders for glaze were pulverized using an automatic pulverizer (HERZOG HSM-250A at AIST Tsukuba Central 7) and fine-grained fractions were separated by decantation. The fine-grained powders were hot pressed by a multi-purpose high temperature furnace (Fuji Dempa High Multi 10000 at AIST Chubu). To determine the condition for fabrication, several fractions of particle size from a few hundred nm to 1 micrometer were prepared. Experiments were carried out at temperatures of 1000-1150°C and pressures of 40-100 MPa. For comparison, we have also carried out a sintering at the atmospheric pressure after formation.

Fabrication of dense albite aggregate is difficult due to the lower diffusion coefficient and melting temperature. The run products were partially melted in the experiments at the temperatures higher than 1100°C. The run products were porous and were not completely sintered in the experiments using powders with particle size of 1 micrometer. Even in the experiments using powders using a few hundred nm, it takes about a hundred hours to fabricate dense aggregate under the pressure of 40 MPa and the temperature of 1100°C, although the materials were partially melted. We succeeded to fabricate dense aggregate without melt phase in the experiment using powders with particle size of a few hundred nm under the pressure of 100 MPa and the temperature of 1080 °C for 36 hours.

Above mentioned results indicate that using fine particle size less than a few hundred nm, temperature of around 1080°C and the pressure above 100 MPa are essential for dense fabrication. There is a possibility that microstructures of aggregate controls the complicated transient behaviors expected for albite. We further explore the method to fabricate the aggregates with various microstructures.

Keywords: albite feldspar, hot pressing, fabrication, sintering

## Fluid flow governed by fault zone architecture, the Alpine Fault, New Zealand

\*Norio Shigematsu<sup>1</sup>, Cecile Massiot<sup>2</sup>, John Townend<sup>2</sup>, Mai-Linh Doan<sup>3</sup>, David D. McNamara<sup>4</sup>, Virginia Toy<sup>5</sup>, Rupert Sutherland<sup>2</sup>, DFDP-2 Science Team

1. Research Institute of Earthquake and Volcano Geology, Geological Survey of Japan, National Institute of Advanced Industrial Science and Technology, 2. Victoria University of Wellington, 3. University of Grenoble, 4. National University of Ireland, Galway, 5. University of Otago

Fracture pattern within a fault zone controls and records a wide range of crustal processes. However, these fractures usually reflect the complicated history of reactivation, and it is difficult to reveal how the fractures were formed. The Alpine Fault provides a unique opportunity to overcome this problem because the hangingwall uplift rate is very rapid, implying that all fractures in the hangingwall have not experienced the fault reactivation (e.g., Little, et al., 2005).

The DFDP-2B borehole was drilled in late 2014 in the hangingwall of the Alpine Fault and a series of wireline logging was acquired (Sutherland et al., 2015). The orientations of planar structures in the hangingwall of the Alpine Fault were revealed by the analysis of acoustic borehole televiewer (BHTV) logs (Massiot et al., 2017). In this study, fracture pattern near the Alpine Fault was examined based on the orientations of fractures revealed by the BHTV logs. Unfortunately, drillcore samples were not recovered due to technical problems during the drilling.

Fractures were formed or slipped in response to ambient stress. In this study, a technique of stress tensor inversion was applied to the orientations of fractures to characterise the fracture pattern. Reduced stress tensors were inferred with assuming the Wallace-Bott hypothesis based on fault slip data. Different fracture patterns should yield different solutions of reduced stress tensor. However, fracture orientation based on BHTV are not usually complete fault slip data without slip directions, although truncated features in BHTV logs occasionally constrain slip directions. For this reason, we compute stress parameters using the Hough transform method (Yamaji et al., 2006). We assume that fractures with similar geometries to the Alpine Fault accommodated similar top-to-the-west shear, and that other fractures have reverse fault components.

2244 planar structures were detected in BHTV logs, and 1680 of them can be interpreted as fractures. Stress tensors were determined for groups of fractures within 20 m depth intervals. The analyses in depth intervals shallower than 730 m (measurement depth) yield orientations (trend/plunge) for the maximum and minimum compressive stress axes  $S_1$  and  $S_3$  of about 120/20 and 020/30 ( $\pm 30^\circ$ ), respectively and a stress ratio of  $(S_2 - S_3)/(S_1 - S_3) = 0.3 - 0.4$ , while those in depth intervals deeper than 730 m yield  $S_1$  and  $S_3$  axes of about 310/10 and 050/45 ( $\pm 30^\circ$ ), respectively and a stress ratio of  $(S_2 - S_3)/(S_1 - S_3) = 0.7$ . Solution of stress tensor, i.e., fracture pattern, changes at  $\sim 730$  m depth. The thermal profile measured by distributed temperature sensing (DTS) using a fibre-optic cable indicates that a thermal gradient also changes at  $\sim 730$  m depth.

The dataset of fractures deeper than 730 m characteristically includes shallowly SE dipping structures. Orientations of these structures correspond to the  $R_1$  shear of the Alpine Fault, which are often developed in fault damage zones. In general, damage zones of fault zones have high permeability compare to the surrounding rocks and fault core (e.g., Cain et al., 1996; Lockner et al., 2009). It can be considered that rock and fluid advectations play key role to account for the thermal profile of DFDP-2B (Sutherland et al., submitted). Therefore, there is a possibility that the deflection in the thermal profile at  $\sim 730$  m depth corresponds to the boundary of the damage zone of the Alpine Fault. The results of fracture pattern and the thermal profile suggest fluid flow governed by the fault zone architecture of the Alpine Fault.

Keywords: fracture pattern, acoustic borehole televiewer, The Alpine Fault, DFDP-2B , stress tensor inversion

## Influence of water fugacity on flow properties of fine-grained anorthite aggregates under the lower crustal conditions

\*Masanori Kido<sup>1</sup>, Jun Muto<sup>1</sup>, Sanae Koizumi<sup>2</sup>, Hiroyuki Nagahama<sup>1</sup>

1. Department of Earth Science, Tohoku University, 2. Earthquake Research Institute, The University of Tokyo

Fluids in deep part of the crust have an important role in deformation and seismicity of the crust. In particular, water has great influence on rheological properties of rocks and minerals. Significant reductions of flow strength caused by water have been discovered for dominant mineral constituents of the crust and mantle (e.g., Griggs and Blacic, 1965). Flow strength is affected by water fugacity which rises sharply under the pressure corresponding to the lower crust. However, experimental data of crustal materials under the lower crustal conditions are insufficient.

In this study, we performed high temperature and high pressure deformation experiments to reveal rheological properties of feldspar under hydrous conditions. Axial compression tests on synthetic polycrystalline anorthite aggregates with 0.5 wt% of water were performed in a Griggs-type solid medium deformation apparatus at temperature of 900 °C and various confining pressures of 0.8-1.4 GPa. Times were changed to investigate the reduction of strength by diffusion of water into samples. Water contents incorporated in the samples were measured by a Fourier-transformed infrared spectroscopy (FTIR) method.

Strengths of wet anorthite tended to decrease with increasing time or strain magnitude. It was suggested that anorthite samples were still not saturated with water in time range of this study. Strengths of wet anorthite also decreased with increasing confining pressures. Differential stresses were significantly lower than predicted values by previous flow laws for wet anorthite obtained by low pressure experiments (<0.5 GPa). This implies that the effect of fugacity of water on strength in higher pressure might be larger than those predicted by lower pressure experiments (e.g., Rybacki et al., 2006). Our experiments show that the strength of hydrous rocks in the lower crust becomes lower than that predicted by previous studies.

Keywords: rheology, water fugacity, fine-grained anorthite aggregates

# Apparent dielectric constants of brines at high P-T conditions: A preliminary report

\*Kenichi Hoshino<sup>1</sup>, Yuika Morita

1. Department of Earth and Planetary Systems Science, Hiroshima University

Common geofluids may be mixed solvents of water and salt(s) with occasional gas species. A difference in chemical potentials of a jth solute ( $D\mu_j^\circ$ ) in water and in the mixed solvent may be expressed as:

$$D\mu_j^\circ = \omega_j (1/\varepsilon_m - 1/\varepsilon_w),$$

where,  $\omega_j$  is the Born coefficient of the solute and  $\varepsilon_m$  and  $\varepsilon_w$  are the dielectric constants of the solvent and water, respectively. Therefore, the constant is a key parameter characterizing chemical properties of the solvent. In other words, we may obtain state quantities of solutes in any mixed solvent from those in water such as derived by SUPCRT92 when the constant of the solvent is known.

Numerous experiments of quartz solubility measurements at high P-T conditions have revealed that salting-in and -out effects occur in H<sub>2</sub>O-NaCl solutions. The effects could be explained by the above difference in the chemical potentials of dissolved Si, mainly as SiO<sub>2(aq)</sub>, in water and in the solution. In the most experiments at P = 50 - 200 MPa, T = 200 - 550°C with NaCl molalities as 0.5 - 1.6, quartz solubilities are higher than those in water, that is, the salting-in occurs in the conditions.

A simple formula to estimate apparent dielectric constants of 1 molal NaCl solutions at P = 50 - 200 MPa and T = 25 - 550°C has been obtained from the above quartz solubility data with an empirical equation for the dielectric constants of the solution at low temperatures (< 50°C). A ratio of the constants of the solution to water,  $\varepsilon_b / \varepsilon_w$  at any P-T condition in the above range can be written simply by a Gaussian function as:

$$\varepsilon_b / \varepsilon_w = a / (2\pi b)^{0.5} \exp(-(T - c)^2 / (2b)) + d,$$

where,  $\pi$  and T are the ratio of the circumference of a circle to its diameter and a temperature in Kelvin, and a, b, c and d are constants as 300, 13000, 573 and 0.8, respectively. The equation implies that the salting-in effect is highest at around 300°C and vanishes at around 100 and 500°C.

Preliminary calculations of quartz precipitation from quartz saturated water and from the 1 molal NaCl solution with decreasing temperatures from 500 to 200°C at 100 MPa show that the amount of precipitation from water during a step of 25°C-decreasing temperature is largest at around 400°C (425 - 400°C), but is only 30% larger than that at 475°C, while it from the latter solution is largest at around 350°C, and is 9 times larger than at 475°C. The results suggest that brine-rock interactions with decreasing temperatures may be enhanced extremely at around 350°C.

Keywords: dielectric constant, brine, water-rock interaction

## Three-dimensional geofluid distribution of Kii Peninsula, SW Japan

\*Yusuke Kinoshita<sup>1</sup>, Yasuo Ogawa<sup>1</sup>, Zenshiro Saito<sup>1</sup>, Rina Noguchi<sup>1</sup>, Kiyoshi Fuji-ta<sup>2</sup>, Satoru Yamaguchi<sup>3</sup>, Umeda Koji<sup>4</sup>, Koichi Asamori<sup>5</sup>, Masahiro Ichiki<sup>6</sup>

1. Tokyo Institute of Technology, 2. Osaka University, 3. Osaka City University, 4. Hirosaki University, 5. Japan Atomic Energy Agency, 6. Touhoku University

Although Kii peninsula is located in the forearc side of southwest Japan, it has high temperature hot springs and fluids from mantle are inferred from the isotopic ratio of helium. Non-volcanic tremors underneath the Kii Peninsula suggest rising fluids from slab.

Previously, in the southern part of the Kii Peninsula, wide band magnetotelluric measurements were carried out (Fujita et al., 1997; Umeda et al., 2004). These studies could image the existence of the conductivity anomaly in the shallow crust and in the deep crust. Long period observation using network MT data showed low resistivity on wedge mantle (Yamaguchi et al., 2009). These studies, however, used two dimensional inversions and three-dimensionality is not fully taken into consideration.

As part of the “Crustal Dynamics” project, we have measured 20 more stations so that the whole wide-band MT stations constitute grids to make three-dimensional modeling of the area.

In total we have wide-band magnetotelluric sites. Preliminary 3d inverse modeling showed the following features.

- (1) The high resistivity in the eastern Kii Peninsula at depths of 5-40km. This may imply consolidated magma body of Kumano Acidic rocks underlain by resistive Philippine Sea Plate which subducts with a low dip angle.
- (2) The northwestern part of Kii Peninsula has the shallow low resistivity in the upper crust.
- (3) The northwestern part of the survey area has a deeper conductor in the lower crust to upper mantle. This reflects the Philippine Sea subduction with higher dip angle.



## 3D magnetotelluric imaging of fluid distribution in a seismogenic region, Miyagi, NE Japan

Zenshiro Saito<sup>2</sup>, \*Yasuo Ogawa<sup>1</sup>, Masahiro Ichiki<sup>3</sup>, Hideyuki Satoh<sup>4</sup>, Yusuke Kinoshita<sup>2</sup>, Atsushi Suzuki<sup>2</sup>, Puwis Amatyakul<sup>1</sup>

1. Volcanic Fluid Research Center, School of Science, Tokyo Institute of Technology, 2. Earth and Planetary Sciences, Tokyo Institute of Technology, 3. Graduate School of Science, Tohoku University, 4. National Institute of Advanced Industrial Science and Technology

Northern Miyagi is located in one of the strain concentration zones in NE Japan. This area is well known to have high seismicity and experienced two large earthquakes, the 1962 Northern Miyagi Earthquake (M6.5) and the 2003 Northern Miyagi Earthquake (M6.2). The 2003 earthquake was well studied and its focal mechanism and aftershock distribution support that the earthquake was a high angle reversed fault, which is a reactivation of an originally normal fault, created in the Miocene during the Japan opening. The surface extension of the fault is recognized as a flexure. Geologically, the area is mostly simply covered with thick sediment and is surrounded by granitic rocks of Kitakami Mountains to the east and to the north. The objective of this study is to image the geofluid in three dimensions and relate them to earthquake activities in the region. The previous studies have done by 2D modeling. We used MT data at 67 sites in total: 39 sites are new, 24 sites of them are arranged in an approximately 2 km grid and other 15 sites are along E-W profile above the focal area of the 2003 Northern Miyagi earthquake, whereas two older dataset were along profiles, one NEE-SWW profile with 16 sites (Mitsuhata et al., 2001), and one NNE-SSW profile with 12 sites (Nagao, 1997). We inverted the data using WS3dMTINV (Siripunvaraporn and Egbert, 2009). The model showed that two shallow (less than 10km depth) and three deep (deeper than 10km) conductors exist: One of shallow conductors represent sedimentary layers. The thickest part is located around Izu-Numa in the northwestern part of the study area. Another is westward dipping conductor as fractured zone of the fault. The hypocenters of the aftershocks of 1962 earthquake distribute at the deeper extension of this dipping conductive layer. deep conductors are located at more 10km depth near the focal area of the 1900, 1962 and 2003 Northern Miyagi earthquake, respectively. The seismic activity is seen at shallower side of the border between itself and high resistivity anomaly. The deep conductors may imply an anomalous body containing saline fluids originating from slab fluids. And, we noticed that seismic activity is high around the deep conductors covered by high-resistivity, especially, along the fault. This may suggest the episodic migration of fluid from the fluid reservoir to the upper brittle crust triggers high seismicity.

Keywords: fluid, electrical resistivity, magnetotellurics, Northern Miyagi Earthquake

## Simultaneous measurements of elastic wave velocity and electrical conductivity in fluid-bearing granitic rocks under confining pressures

\*Yohei Kaiwa<sup>2</sup>, Aya Konno<sup>2</sup>, Erina Deai<sup>2</sup>, Kyara Teranishi<sup>2</sup>, Tohru Watanabe<sup>1</sup>

1. Graduate School of Science and Engineering, University of Toyama, 2. Department of Earth Sciences, University of Toyama

Geophysical mapping of fluids is critical for understanding crustal processes. Seismic velocity and electrical resistivity structures have been revealed to study the fluid distribution. However, the fluid distribution has been still poorly constrained. Observed velocity and resistivity should be combined to make a quantitative inference on fluid distribution. The combined interpretation requires a thorough understanding of velocity and resistivity in fluid-saturated rocks. We have studied elastic wave velocities and electrical conductivity in brine-saturated granitic rocks under confining pressures.

Aji granite (Aji, Kagawa Pref., Japan) and Oshima granite (Oshima, Ehime Pref., Japan) were selected as rock samples for textural uniformity. Cylindrical samples (D=26 mm, L=30 mm) were evacuated and filled with 0.1 M KCl aqueous solution. Velocity and electrical conductivity were simultaneously measured by using a 200 MPa hydrostatic pressure vessel. The pore-fluid was electrically insulated from the metal work by using teflon devices. The confining pressure was progressively increased up to 150 MPa, while the pore-fluid pressure was kept at 0.1 MPa. It took 3 days or longer for the electrical conductivity to become stationary after increasing the confining pressure.

Velocity and conductivity showed reproducibly contrasting changes with increasing confining pressure. Elastic wave velocities increased by less than 10% as the confining pressure increased from 0.1 MPa to 50 MPa, while electrical conductivity decreased by an order of magnitude. The changes must be caused by the closure of cracks under pressure. The large change at low pressures shows that there are lots of cracks with small aspect ratios ( $<10^{-3}$ ). Both velocity and conductivity showed no remarkable changes at higher pressures. The large conductivity change at low pressures must be related to the percolation of cracks.

Keywords: seismic velocity, electrical conductivity, fluid

## Change in electrical conductivity in a brine-saturated granite under uni-axial compression

Ryo Sawaki<sup>2</sup>, \*Tohru Watanabe<sup>1</sup>, Watanabe Shinya<sup>2</sup>

1. Graduate School of Science and Engineering, University of Toyama, 2. Department of Earth Sciences, University of Toyama

Geophysical observations have shown that fluids exist pervasively within the crust. Fluids fill intergrain cracks (open grain boundaries) and intra-grain cracks at the upper and middle crust conditions. Since the opening of cracks strongly depends on the stress state, electrical conductivity should be anisotropic under a stress state. We have conducted uni-axial compression tests on brine-saturated granitic rocks and studied the change in electrical conductivity in the directions parallel and perpendicular to the compression.

The loading system is composed of a hand press (Maximum load: 20 kN), a load cell and stainless steel end-pieces. A fine grained (100-500  $\mu$ m) biotite granite (Aji, Kagawa Pref., Japan) was selected as a rock sample for its small grain size and textural uniformity. A cube sample with the edge length of 25 mm was filled with 0.1 M KCl aqueous solution and loaded up to 20 MPa. Electrical impedance was continuously monitored during a compression test with two-electrode method (Ag-AgCl electrodes).

Electrical conductivity decreased with increasing axial stress in the directions parallel and perpendicular to the compression. Electrical conductivity decreased in both directions with increasing axial stress, and the conductivity change was almost reversible. No significant difference in the magnitude of conductivity change was observed between two directions. The decrease in conductivity must be caused by the closure of cracks, which were perpendicular or subperpendicular to the compression. The fluid path for the electrical conduction in the axial direction must be composed of cracks parallel and perpendicular to the axial stress. Electrical conductivity does not become anisotropic, while elastic wave velocity does.

Keywords: differential stress, electrical conductivity, anisotropy

## Pressure dependence of electrical conductivity in brine-saturated Berea sandstone and its pore structure

\*Minako Nambu<sup>1</sup>, Tohru Watanabe<sup>2</sup>

1. Graduate School of Science and Engineering for Education, University of Toyama, 2. Graduate School of Science and Engineering, University of Toyama

Electrical conductivity in brine-saturated Berea sandstone (porosity ~20%) was measured under confining pressures of up to 100 MPa. The pore-fluid pressure was kept at the atmospheric pressure (0.1 MPa). Electrical conductivity decreased by 22% as the confining pressure was increased to 40 MPa. Volumetric strain of a dry rock sample was separately measured under confining pressures. The volume change was 0.7% as the confining pressure was increased to 50 MPa. The change in porosity should be only 1%. The observed relatively large decrease in conductivity shows that the connectivity of pores in the porous Berea sandstone was significantly reduced by a small decrease in porosity. In order to understand the nature of the conduction path, the pore structure in Berea sandstone was observed with X-ray CT conducted at Tokyo Metropolitan Industrial Technology Research Institute. 3D images of pores were constructed by processing X-ray CT images to examine the connectivity of pores.

Keywords: electrical conductivity, sandstone, pore structure